



**HAL**  
open science

# Copper microRNAs modulate the formation of giant feeding cells induced by the root knot nematode *Meloidogyne incognita* in *Arabidopsis thaliana*

Yara Nouredine, Joffrey Mejias, Martine da Rocha, Sébastien Thomine, Michaël Quentin, Pierre Abad, Bruno Favery, Stéphanie Jaubert-Possamai

## ► To cite this version:

Yara Nouredine, Joffrey Mejias, Martine da Rocha, Sébastien Thomine, Michaël Quentin, et al.. Copper microRNAs modulate the formation of giant feeding cells induced by the root knot nematode *Meloidogyne incognita* in *Arabidopsis thaliana*. *New Phytologist*, 2022, 236 (1), pp.283-295. 10.1111/nph.18362 . hal-03866626

**HAL Id: hal-03866626**

**<https://hal.science/hal-03866626>**

Submitted on 22 Nov 2022

**HAL** is a multi-disciplinary open access archive for the deposit and dissemination of scientific research documents, whether they are published or not. The documents may come from teaching and research institutions in France or abroad, or from public or private research centers.

L'archive ouverte pluridisciplinaire **HAL**, est destinée au dépôt et à la diffusion de documents scientifiques de niveau recherche, publiés ou non, émanant des établissements d'enseignement et de recherche français ou étrangers, des laboratoires publics ou privés.

1

2 **Copper microRNAs modulate the formation of giant feeding cells induced by the root**  
3 **knot nematode *Meloidogyne incognita* in *Arabidopsis thaliana***

4

5

6 Yara Noureddine<sup>1</sup>, Joffrey Mejias<sup>1</sup>, Martine da Rocha<sup>1</sup>, Sébastien Thomine<sup>2</sup>, Michaël  
7 Quentin<sup>1</sup>, Pierre Abad<sup>1</sup>, Bruno Favery<sup>1</sup>, and Stéphanie Jaubert-Possamai<sup>1\*</sup>

8 1 INRAE, Université Côte d'Azur, CNRS, ISA, Sophia Antipolis, F-06903, France

9 2 Institute for Integrative Biology of the Cell (I2BC), UMR9198 CNRS/CEA/Univ. Paris Sud,  
10 Université Paris-Saclay, Gif-sur-Yvette, France.

11 Corresponding author: stephanie.jaubert@inrae.fr

12

13 **Word Count. 5050**

14 Introduction: 1,127 words

15 Materials and Methods: 872 words

16 Results: 1842 words

17 Discussion: 1222 words

18 Acknowledgements: 147 words

19 Number of Tables: 1

20 Number of figures: 5 (all in colors)

21 Supporting information: 10 figures and 10 tables.

22

23 **Heading**

24 *Arabidopsis* copper microRNAs modulate the development of feeding site induced by root  
25 knot nematodes.

26 **Twitter :**

27 @stephejaubert

28 @noureddine\_yara

29 @brunofavery

30 **ORCID :**

31 Stéphanie Jaubert-Possamai : <https://orcid.org/0000-0002-3518-727X>

32 Yara Noureddine : <https://orcid.org/0000-0002-6875-5835>

33 Joffrey Mejias : <https://orcid.org/0000-0001-7663-0314>

34 Martine da Rocha : <https://orcid.org/0000-0003-0959-2295>

35 Sébastien Thomine : <https://orcid.org/0000-0003-0045-1701>

36 Michaël Quentin : <https://orcid.org/0000-0002-8030-1203>

37 Pierre Abad : <https://orcid.org/0000-0003-0062-3876>

38 Bruno Favery : <https://orcid.org/0000-0003-3323-1852>

39

40 **Summary** (161 words)

- 41
- 42 • Root-knot nematodes (RKN) are root endoparasites that induce the dedifferentiation of a  
43 few root cells and the reprogramming of their gene expression to generate giant  
44 hypermetabolic feeding cells.
  - 45 • We identified two microRNA families, miR408 and miR398, as upregulated in  
46 *Arabidopsis thaliana* and *Solanum lycopersicum* roots infected by root-knot nematodes.  
47 In plants, the expression of these two conserved microRNA families is known to be  
48 activated by the SPL7 transcription factor in response to copper starvation.
  - 49 • By combining functional approaches, we deciphered the network involving these  
50 microRNAs, their regulator and their targets. *MIR408* expression was located within  
51 nematode-induced feeding cells like its regulator *SPL7* and was regulated by copper.  
52 Moreover, infection assays with *mir408* and *spl7* KO mutants or lines expressing targets  
53 rendered resistant to cleavage by miR398 demonstrated the essential role of the  
54 *SPL7/MIR408/MIR398* module in the formation of giant feeding cells.
  - 55 • Our findings reveal how perturbation of plant copper homeostasis, *via* the  
56 *SPL7/MIR408/MIR398* module, modulates the development of nematode-induced  
57 feeding cells.

57

58

59 Key words: root-knot nematodes, microRNAs, copper, signaling, *Arabidopsis*

## 60 **Introduction**

61 MicroRNAs are small non-coding RNAs that regulate the expression of protein-coding genes,  
62 mostly at the post-transcriptional level, in plants. They are major post-transcriptional regulators  
63 of gene expression in various biological processes, including plant development (Li and Zhang,  
64 2016), responses to abiotic stresses (Barciszewska-Pacak *et al.*, 2015), hormone signalling  
65 (Curaba *et al.*, 2014), and responses to pathogens or symbiotic micro-organisms (Hoang *et al.*,  
66 2020; Weiberg and Jin, 2015). MicroRNAs and short interfering RNAs (siRNAs) were recently  
67 shown to play a key role in plant-pathogen crosstalk through trans-kingdom RNAi processes  
68 (Weiberg *et al.*, 2013; Cai *et al.*, 2018; Dunker *et al.*, 2020). MicroRNAs are produced by the  
69 cleavage of long double-stranded RNA precursors by the DICER RNase, generating 20-22  
70 nucleotides miRNA duplexes composed of a mature (5P) and a complementary (3P) strand.  
71 One of the two strands is then incorporated into the RNA-induced silencing complex (RISC) to  
72 guide the major RISC protein, ARGONAUTE1 (AGO1), to the targeted messenger RNA  
73 (mRNA) on the basis of sequence complementarity. The hybridization of AGO1-bound  
74 miRNAs to their targets induces predominantly targeted mRNA degradation in plants, but it  
75 may also lead to an inhibition of mRNA translation (Axtell, 2013).

76 The miR408 and miR398 microRNA families are conserved so-called “copper microRNAs”,  
77 due to their function in the plant response to copper deficiency (Zhang *et al.*, 2015; Yamasaki  
78 *et al.*, 2007). Copper is an essential nutrient for plants, due to its function as a cofactor for many  
79 proteins. Copper proteins are involved in electron transport chains or function as enzymes in  
80 redox reactions. In plants, copper is involved in respiration, photosynthesis, ethylene  
81 perception, the metabolism of reactive oxygen species and cell wall remodelling (reviewed in  
82 Burkhead *et al.*, 2009). Copper microRNAs accumulate in response to copper deficiency and  
83 their synthesis is repressed when copper concentrations are sufficiently high (Yamasaki *et al.*,  
84 2009). The underlying mechanism has been described in *Arabidopsis thaliana*, in which the  
85 regulation of *MIR408*, *MIR398B* and *MIR398C* by copper levels was shown to be mediated by  
86 the SQUAMOSA PROMOTER-BINDING PROTEIN-LIKE7 (SPL7) transcription factor  
87 (Yamasaki *et al.*, 2009). The *A. thaliana* genome contains a single copy of *MIR408*, and three  
88 *MIR398* genes: *MIR398A*, *-B* and *-C*. At high copper concentrations, the DNA-binding activity  
89 of the SPL7 transcription factor is repressed, preventing the induction of transcription for  
90 downstream genes, such as *MIR408* or *MIR398B* and *MIR398C*, but not *MIR398A* (Sommer *et al.*  
91 *et al.*, 2011; Yamasaki *et al.*, 2009). In the presence of low concentrations of copper, SPL7  
92 activates the expression of copper-responsive microRNAs that target and repress the expression

93 of genes encoding copper-binding proteins. These proteins are replaced by proteins that do not  
94 bind copper, to save copper resources for the functions for which this element is essential, such  
95 as photosynthesis (reviewed in Burkhead *et al.*, 2009). For example, the mRNA for the cytosolic  
96 COPPER/ZINC (Cu-Zn) SUPEROXIDE DISMUTASE, CSD1, which can be replaced by an  
97 iron (Fe)-dependent SOD, is targeted by the copper microRNA miR398. In addition to their  
98 regulation as a function of copper levels through the activity of SPL7, *MIR408* and the *MIR398*  
99 family are also regulated by several environmental cues and abiotic stresses, such as light,  
100 which regulates *MIR408* activity through the ELONGATED HYPOCOTYL5 (HY5) or  
101 PHYTOCHROME INTERACTING FACTOR1 (PIF1) transcription factors in *A. thaliana*  
102 (Jiang *et al.*, 2021), and salinity, oxidative and cold stresses, which have been shown to induce  
103 *MIR408* in *A. thaliana* (Ma *et al.*, 2015), or cadmium treatment in *Brassica napus* (Fu *et al.*,  
104 2019). The miR408 and miR398 families have been widely analysed in plant responses to  
105 abiotic stresses, but little is known of their role in plant responses to biotic stresses. In sweet  
106 potato, *MIR408* has been associated with plant defences, as it is repressed by jasmonic acid  
107 (JA) and wounding, and miR408-overexpressing plants have attenuated resistance to insect  
108 feeding (Kuo *et al.*, 2019). Moreover, miR398 has been shown to regulate cell death in response  
109 to the causal agent of barley powdery mildew, *Blumeria graminis* (Xu *et al.*, 2014).

110 Root-knot nematodes (RKN) of the genus *Meloidogyne* are obligatory sedentary plant parasites  
111 capable of infesting more than 5,000 plant species (Abad and Williamson, 2010; Blok *et al.*,  
112 2008). The RKN larvae penetrate the roots, in which they induce the de-differentiation of five  
113 to seven parenchyma root cells and their reprogramming into the multinucleate, hypertrophied  
114 feeding cells that form the feeding site. These metabolically overactive feeding cells provide  
115 the nutrients required for RKN development (Favery *et al.*, 2020). During the dedifferentiation  
116 of vascular cells and their conversion into ‘giant’ feeding cells, the cells surrounding the feeding  
117 site begin to divide again. The growth of the feeding cells and the division of the surrounding  
118 cells lead to a root swelling known as a gall. The feeding cell induction occurs in the first three  
119 days after root infection. Feeding cell formation can be split into two phases. Firstly, the cells  
120 undergo successive nuclear divisions coupled with cell expansion until ten days post infection  
121 (dpi) in *A. thaliana* (Caillaud *et al.*, 2008). In the second phase, from 10 to 21 dpi, the successive  
122 nuclear divisions stop and the nuclei of the feeding cells undergo extensive endoreduplication  
123 (Wiggers *et al.*, 1990; de Almeida Engler and Gheysen, 2013). The dedifferentiation of vascular  
124 cells and their conversion into giant cells result from an extensive reprogramming of gene  
125 expression in root cells, in response to RKN signals. In *A. thaliana*, the expression of

126 approximately 10% of protein-coding genes is modified in galls induced by RKN (Cabrera *et*  
127 *al.*, 2014; Yamaguchi *et al.*, 2017; Jammes *et al.*, 2005; reviewed in Escobar *et al.*, 2011). The  
128 sequencing of small RNAs identified 24 mature microRNAs differentially expressed (DE)  
129 between *A. thaliana* galls induced by *M. incognita* and uninfected roots at 7 and 14 dpi and 62  
130 microRNAs DE at 3 dpi (Medina *et al.*, 2017; Cabrera *et al.* 2015). The miR408 and miR398  
131 families of copper-responsive microRNAs were found to be upregulated in galls at 7 and/or 14  
132 dpi.

133 In this article, we showed a conserved upregulation of these two microRNA families in  
134 *Arabidopsis* and tomato galls. Moreover, we found that the upregulation of *MIR408* in response  
135 to RKN was required for successful infection. Our findings highlighted a strong activity of the  
136 *MIR408* promoter (*pMIR408*) in early galls that is i) driven by the modulation of environmental  
137 copper levels, ii) **is localised in the same gall tissue than the strong *SPL7* expression.**  
138 Moreover, we also demonstrated that this transcription factor helps to promote giant cell  
139 development. In addition, we showed that the silencing of *CSD1* and *BLUE COPPER*  
140 *BINDING PROTEIN (BCBP)* transcripts by miR398 is involved in gall development. Finally,  
141 the watering of *Arabidopsis* with copper sulphate solutions at concentrations below the toxicity  
142 thresholds for nematode and plant development greatly decreased the RKN infection and  
143 impaired feeding cell development.

144

## 145 **Material and Methods**

### 146 **Biological material, growth conditions and nematode inoculation**

147 Seeds of *A. thaliana* Col0 and mutants *mir408-1* (SALK\_038860), *mir408-2*  
148 (SALK\_121013.28.25.n), *spl7* (SALK\_093849), *mcsd1* and *mbcbp* (Beauclair *et al.*, 2010),  
149 *pmiR408::GUS* (Zhang *et al.*, 2013) and *pSPL7::GUS* (Yamasaki *et al.*, 2009) were surface-  
150 sterilised and sown on Gamborg B5 medium agar plates (0.5 x Gamborg, 1% sucrose, 0.8%  
151 agar, pH 6.4). The plates were incubated at 4°C for two days, then transferred to a growth  
152 chamber (20°C with an 8 h light/ 16 h darkness cycle). *M. incognita* strain “Morelos” was  
153 multiplied on tomato plants in a growth chamber (25°C, 16 h light/8 h darkness). For the RKN  
154 infection of plants in soil, two-week-old plantlets grown *in vitro* were transferred to a mixture  
155 of 50% sand (Biot B5)/50% soil in a growth chamber (21°C, 8 h light/16 h darkness). For  
156 studies of the effect of copper on gall development on plants *in vitro*, *Arabidopsis* plantlets were  
157 sown and cultured *in vitro*, as described above, on Gamborg B5 medium supplemented with 50  
158 µM CuSO<sub>4</sub>.

159 **Root knot nematode infection assay**

160 For nematode infections *in vitro*, second-stage juveniles (J2s) were surface-sterilised with  
161 HgCl<sub>2</sub> (0.01%) and streptomycin (0.7%), as described by Caillaud and Favery (2016). We  
162 inoculated each 25-day-old seedling grown individually *in vitro* with 200 sterilised J2s  
163 resuspended in Phytigel (5%). Infection assays were performed on *Arabidopsis* mutants and a  
164 wild-type ecotype in soil. We inoculated 20 to 30 two-month-old plantlets with 150 J2s per  
165 plant and incubated them in a growth chamber (21°C, 8 h light/16 h darkness). Seven weeks  
166 after infection, the roots were collected, washed in tap water and stained with eosin (0.5 %).  
167 Stained roots were weighed and galls and egg masses were counted on each root under a  
168 binocular microscope. Mann and Whitney tests (2.5%) were performed to determine the  
169 significance of the observed differences in the numbers of egg masses and galls per root.

170 **Small RNA sequencing from galls and uninfected tomato roots**

171 Biological material, RNA extraction, small RNA and RNA sequencing, read mapping and  
172 statistical analysis are presented as supporting informations (Method S1-S6).

173 **BABB clearing**

174 Feeding site development was evaluated by the BABB clearing method described by Cabrera  
175 *et al.*, (2018). Briefly, the area occupied by the giant cells was measured on galls collected  
176 seven weeks post infection, cleared in benzyl alcohol/benzyl benzoate (BABB) and examined  
177 under an inverted confocal microscope (model LSM 880; Zeiss). Zeiss ZEN software was used  
178 to measure the area occupied by the giant cells in each gall, on two biological replicates. Data  
179 were analysed in Mann and Whitney tests.

180 **Copper treatment**

181 *M. incognita* eggs were collected as previously described (Caillaud and Favery, 2016) and  
182 placed on a 10 µm-mesh sieve for hatching in tap water. Free-living J2s were collected from  
183 the water with a 0.5 µm-mesh sieve. We evaluated the toxicity of copper to J2s by incubating  
184 freshly hatched J2s in solutions of copper sulphate of various concentrations for 24 hours. The  
185 numbers of living or dead J2s were then determined by counting under a binocular microscope.  
186 We investigated the effects of copper on plant-nematode interactions in *Arabidopsis* Col0  
187 grown in soil. *Arabidopsis* Col0 plantlets were prepared and inoculated as previously described  
188 for in-soil infection. Half the plants were watered with 50 µM CuSO<sub>4</sub> two days after inoculation  
189 with J2s and then once per week for the next seven weeks. Control Col0 plants were watered  
190 with tap water in place of copper sulphate solution, at the same frequency. Seven weeks after

191 inoculation, the plants were collected, their roots were washed and weighed, and the numbers  
192 of galls and egg masses on the roots were counted, as described above.

### 193 **Studies of promoter-GUS fusion gene expression**

194 We localised the promoter activity of *MIR408* and *SPL7* in *A. thaliana* lines expressing various  
195 fusions of the *GUS* reporter gene to promoters from these genes. We inoculated 21-day-old  
196 seedlings in soil and *in vitro*, as described above. We collected inoculated roots and washed  
197 them in water, 3, 7, 14 and 21 dpi. GUS staining was performed as previously described (Favery  
198 *et al.*, 1998), and the roots were observed under a Zeiss Axioplan 2 microscope. Stained galls  
199 were dissected, fixed by incubation in 1% glutaraldehyde and 4% formaldehyde in 50 mM  
200 sodium phosphate buffer pH 7.2, dehydrated, and embedded in Technovit 7100 (Heraeus  
201 Kulzer, Wehrheim, Germany), according to the manufacturer's instructions. Sections were cut  
202 and mounted in DPX (VWR International Ltd, Poole, UK), and observed under a Zeiss  
203 Axioplan 2 microscope (Zeiss, Jena, Germany).

### 204 **Bioinformatic analysis**

205 We used psRNA target with default parameters for the prediction of miR408 targets (Dai,  
206 Zhuang and Zhao 2018).

### 207 **Quantitative PCR**

208 Total RNA was extracted from galls and uninfected roots produced in soil with the miRNeasy  
209 kit (QIAGEN) according to the manufacturer's instruction. 500ng of total RNA were subjected  
210 to reverse transcription with the Superscript IV reverse transcriptase (Invitrogen). qPCR  
211 analyses were performed as described by Nguyen *et al.* (2018). We performed qPCR on  
212 triplicate samples of each cDNA from three independent biological  
213 replicates. *OXA1* (*At5g62050*) and *UBP22* (*AT5G10790*) were used for the normalization of  
214 qRT-PCR data. Quantifications and statistical analyses were performed with SATqPCR  
215 (Rancurel *et al.*, 2019), and the results are expressed as normalized relative quantities. Primers  
216 used to amplify the premiRNAs and the transcripts are listed in Table S1.

217

### 218 **NBT staining of galls**

219 Biological material, and NBT staining of galls are presented as supporting information (Method  
220 S7).

## 221 Results

### 222 **MIR408 is induced in galls and its expression is driven by modulation of copper level**

223 Previous sequencing analyses of microRNAs expressed in *Arabidopsis* galls induced by *M.*  
224 *incognita* revealed an upregulation of mature miR408 in *Arabidopsis* galls at 7 and 14 dpi,  
225 whereas miR398b/c was specifically upregulated in galls at 14 dpi. None of these microRNAs  
226 were shown as DE in galls at 3 dpi produced from young *in vitro* plantlets (Cabrera *et al.* 2016).  
227 Sequencing of small RNAs from uninfected roots and galls of *Solanum lycopersicum* showed  
228 that these two microRNA families were also upregulated in tomato galls at 7 and 14 dpi (Table  
229 1 and Table S2). Therefore, these microRNAs are among the very few conserved microRNAs  
230 which expression profile is conserved in *Arabidopsis* and tomato galls. We investigated the  
231 induction of *MIR408* in response to nematode infection, by inoculating plants expressing  
232 pMIR408::GUS (Zhang and Li, 2013) grown *in vitro* on Gamborg B5 with *M. incognita* J2s.  
233 We observed a strong GUS signal in developing galls at 3 and 7 dpi (Fig. 1a-b). This signal had  
234 decreased in intensity by 14 dpi (Fig. 1c) and disappeared completely from fully developed  
235 galls at 21 and 28 dpi (Fig. S1). On gall sections, the GUS signal was localised in the giant  
236 feeding cells and neighbouring cells, at the 3 dpi, 7 dpi and 14 dpi time points (Fig. 1d-f).  
237 Overexpression of *MIR408* at 7 dpi was confirmed by qPCR analysis of level of premiR408 in  
238 galls at 7 and 14 dpi (Fig S2). The discrepancy between mature miR408 and premiR408 level  
239 in galls at 14 dpi may be explained by the delay between transcription of premiRNA and its  
240 processing into mature microRNA by Dicer as it has been previously described (Thompson *et*  
241 *al.*, 2006; Hutvagner *et al.*, 2001; Schulman *et al.*, 2005). MiR408 is known as a copper  
242 microRNA. To investigate if copper modulation regulates *MIR408* expression in galls,  
243 pMIR408::GUS activity was followed in plants grown *in vitro* with a high copper concentration  
244 (Gamborg B5 plus 5  $\mu$ M CuSO<sub>4</sub>). By contrast to plants grown in Gamborg B5, in plants grown  
245 in the presence of high copper concentrations, the GUS signal was much weaker in galls at 3  
246 and 7 dpi (Fig. 1g-h and 1j-k), and undetectable in galls at 14 dpi (Fig. 1i and 1l). The repression  
247 of *MIR408* expression in galls by high copper concentrations indicates that *MIR408* expression  
248 within *Arabidopsis* galls is regulated by modulation of copper levels.

249

### 250 **The copper microRNA miR408 is crucial for the *Arabidopsis*-*Meloidogyne* interaction**

251 We investigated the role of miR408 in gall development using two previously described  
252 *Arabidopsis* knockout (KO) mutant lines: *mir408-1* and *mir408-2* (Maunoury and Vaucheret,

253 2011). The KO lines and corresponding wild-type plants were inoculated with *M. incognita* J2s  
254 and their susceptibility was quantified by counting the galls and egg masses produced by adult  
255 females at the root surface. The two KO lines for *MIR408* had 40 to 50% fewer galls and egg  
256 masses than the wild type ( $p < 0.05$ ; Fig. 2 and Table S3). The roots of these KO lines were of  
257 similar weight and global architecture to those of wild-type plants (Fig. S2 and Table S3). We  
258 then investigated the effect of the *MIR408* mutation on feeding site development, by comparing  
259 the area of feeding cells within galls collected from KO and wild-type plants (Fig. 2a-c and  
260 Table S3). Both KO mutants had a significantly smaller feeding site area than the wild type.  
261 Overall, these results demonstrate that *MIR408* helps to promote feeding cell development in  
262 the *Arabidopsis*-nematode interaction, and that the lower susceptibility of the *miR408* KO lines  
263 is due to defects of feeding site development.

264 We investigated the targeted transcripts by which miR408 modulates feeding cell development  
265 in galls. The psRNA target algorithm (Dai *et al.*, 2018) predicted 101 genes as putative targets  
266 of miR408 in *Arabidopsis* (Table S4a). The expression profiles of these genes in galls at 7 dpi  
267 and 14 dpi were obtained from previous transcriptome analyses (Jammes *et al.* 2005). Only  
268 seven of the 101 putative targets were differentially expressed in galls at 7 and/or 14 dpi, and  
269 only two putative targets were repressed: a transcript encoding a copper-binding protein,  
270 UCLACYANIN2 (*UCC2*, *At2g44790*), which is known to be cleaved by the RNA INDUCED  
271 SILENCING COMPLEX (RISC) guided by miR408 in senescing leaves and siliques (Thatcher  
272 *et al.*, 2015), and a transcript encoding a PHOSPHATASE 2G (*PP2CG1*, *At2g33700*) (Table  
273 S4b). The repression of these two genes was confirmed in galls at 14 dpi by qPCR (Fig. S3 and  
274 Table S5) supporting that mature miR408 induced the cleavage of these two targets at this time  
275 point.

276

### 277 **SPL7 is an activator of *MIR408* transcription in galls**

278 The regulation of *MIR408* by modulation of copper levels has been shown to be mediated by  
279 the *SPL7* transcription factor (Zhang *et al.*, 2014; Bernal *et al.*, 2012). Transcriptome analyses  
280 from *Arabidopsis* galls showed that *SPL7* was expressed in galls at 7, 14 and 21 dpi (Jammes  
281 *et al.*, 2005). We further investigated the expression of *SPL7* within galls, by inoculating a  
282 *pSPL7::GUS Arabidopsis* line (Araki *et al.*, 2018) with *M. incognita* in the presence of a normal  
283 copper concentration. *SPL7* promoter activity was observed within the gall from 3 to 14 dpi,  
284 with lower levels at 14 dpi (Fig. 3a-c). As observed for *pMIR408::GUS*, sections of

285 *pSPL7::GUS* galls revealed a GUS signal in the giant feeding cells and neighbouring cells (Fig.  
286 3d). We investigated the putative function of *SPL7* in plant responses to RKN, by inoculating  
287 the *Arabidopsis spl7* KO mutant described by Zhang *et al.* (2014) with *M. incognita* J2s. *SPL7*  
288 knockout led to the production of smaller numbers of galls and egg masses per plant than were  
289 observed for the wild-type (Fig. 3e-f and Table S6). This knockout had no effect on root weight  
290 (Fig. S4 and Table S6). Measurements of the area of the feeding site within galls revealed  
291 defects of feeding site formation in the *spl7* mutants, resulting in smaller giant cells than were  
292 observed in wild-type plants (Fig. 3g and Table S6). Overall, these results demonstrate the  
293 requirement of miR408 and *SPL7* for the proper development of giant cells. The upregulation  
294 of mature miR408 observed in galls suggests an induction of *MIR408* expression driven by  
295 *SPL7* due to a decrease in copper availability within the gall.

### 296 **micro398, a second copper-responsive microRNA family involved in the *Arabidopsis-*** 297 ***Meloidogyne* interaction**

298 MiR408 is not the only copper-responsive microRNA reported differentially expressed in galls.  
299 The expression of *MIR398B* and *MIR398C*, from the conserved miR398 family, has also been  
300 shown to be induced in response to copper deficiency, via *SPL7* activity (Araki *et al.*, 2018).  
301 We previously described an induction of the mature miR398b and miR398c in *Arabidopsis*  
302 galls at 14 dpi by sequencing (Medina *et al.*, 2017). However, quantification of the precursors  
303 by qPCR did not confirm the induction of the mature miR398s (Fig S5 and Table S7). Three  
304 targets of the miR398 family have been biologically validated: the *At1g08830* and *At2g28190*  
305 transcripts encoding two copper superoxide dismutases, *CSD1* and *CSD2*, respectively, and the  
306 *At5g20230* transcript encoding the blue copper binding protein (BCBP), identified as a non-  
307 canonical target of miR398 (Brousse *et al.*, 2014). Previous analyses of *Arabidopsis* gall  
308 transcriptome showed a repression of *CSD1* at 7 dpi and of *BCBP* at 7 and 14 dpi while *CSD2*  
309 was not differentially expressed (Jammes *et al.* 2005). qPCR did not confirm the repression of  
310 *CSD1* and *CSD2* and showed a repression of *BCBP* at 7 dpi but with a pvalue of 0.07 (Fig. S5  
311 and Table S7). Despite the lack of confirmation of sequencing and microarray results by qPCR,  
312 we investigated the role of miR398 further, by infecting *Arabidopsis* lines expressing modified  
313 versions of *CSD1* (*mcsd1*) or *BCBP* (*mcbcp*) mRNAs rendered resistant to cleavage by miR398  
314 (Brousse *et al.*, 2014; Beauclair *et al.*, 2010). The target mRNA levels is therefore artificially  
315 increased in these plants. The prevention of *CSD1* transcript cleavage by miR398 had no effect  
316 on root weight (Fig. S6), but led to lower levels of nematode infection, with the mutant having  
317 less galls and egg masses than the wild type (Fig. 4 and Table S8). The *mcbcp* line also had

318 fewer egg masses than the wild-type (Fig. 4 and Table S8). No defect of feeding cell formation,  
319 such as slower feeding cell growth, was observed in either of these lines (Fig. 4 and Table S8).  
320 The specific decrease in egg mass production by females provides evidence for a role for  
321 miR398 in the functionality of feeding cells, although the mutations in the *mcsdl* and *mbcbp*  
322 lines did not affect feeding site size (Fig. 4). These findings demonstrate that the cleavage of  
323 *CSDI* and *BCBP* transcripts by the RISC guided by miR398 helps to promote parasitism.

#### 324 **Modulation of copper levels is essential for plant-RKN interaction**

325 To study further the effect of copper on nematode infection, we analysed the direct effects of  
326 copper on nematode survival and gall development. Free-living *M. incognita* J2s were  
327 incubated in several concentrations of copper sulphate (50  $\mu$ M to 2 mM) used in previous  
328 studies assessing the effect of copper on plant development (Schulten *et al.*, 2019). As a  
329 negative control, J2s were incubated in tap water. Living J2 counts after 24 hours in the copper  
330 sulphate solution showed that copper was non-toxic at a concentration of 50  $\mu$ M (Fig. S7 and  
331 Table S9). By contrast, toxic effects were observed for all other concentrations tested (0.5 mM,  
332 1 mM and 2 mM). We then analysed the effect of copper on gall formation in Col0 and  
333 *pMIR408::GUS* plants grown in soil watered with 50  $\mu$ M CuSO<sub>4</sub>. We also minimised J2s  
334 exposure to copper in the soil, by beginning to water plants 50  $\mu$ M CuSO<sub>4</sub> two days after  
335 inoculation, after the J2s had already penetrated the roots. Watering with 50  $\mu$ M CuSO<sub>4</sub>  
336 repressed pMIR408 activity in uninfected roots and in galls as it can be observed by the  
337 reduction of the GUS signal (Fig. S8) confirming the effects of such treatment in galls. Watering  
338 with 50  $\mu$ M CuSO<sub>4</sub> had no visible effect on root weight and architecture (Fig. S9 and Table  
339 S10), but it resulted in a strong and significant decrease in the number of galls and egg masses  
340 relative to control plants watered with tap water (Fig. 5). Copper is involved in many processes  
341 in plants like the production of reactive oxygen species (ROS). Watering plants with CuSO<sub>4</sub>  
342 may therefore have additional effects in addition to the repression of the *pMIR408* activity. The  
343 effect of watering with CuSO<sub>4</sub> on ROS production during the nematode infection was analysed.  
344 The O<sup>2-</sup> accumulation was followed by Nitro Blue Tetrazolium (NBT) staining of galls collected  
345 14 dpi from plants watered with tap water or with 50  $\mu$ M CuSO<sub>4</sub>. NBT staining showed the  
346 same localisation and intensity signal in galls regardless the watering condition. A strong O<sup>2-</sup>  
347 accumulation can be observed in cells surrounding the feeding site when the giant feeding cells  
348 showed no signal (Fig. S10). Altogether, these results demonstrate that perturbation of plant  
349 copper homeostasis modulates miR408 production in galls and interferes with the plant-RKN  
350 interaction.

## 351 **Discussion**

352 RKN induce the formation of similar giant feeding cells in thousands of plant species. The  
353 conservation of the ontogeny and phenotype of nematode-induced feeding cells between  
354 species, strongly suggests that the plant molecular mechanisms manipulated by RKN are widely  
355 conserved across the plant kingdom. Previous transcriptome analyses on various plant species  
356 have shown that the development of galls in roots infected by RKN is associated with a massive  
357 reprogramming of gene expression (reviewed in Escobar *et al.*, 2011). MicroRNAs are small  
358 non-coding RNAs that regulate gene expression at the post-transcriptional level, and some  
359 microRNA families, such as the miR156 and miR167 families, are widely conserved in plants  
360 (Chavez Montes *et al.*, 2014). The role for microRNAs in controlling gene expression during  
361 the formation of galls was recently reported in *Arabidopsis* (reviewed in Jaubert-Possamai *et*  
362 *al.*, 2019), for the conserved microRNAs miR390, miR172 and miR159 (Cabrera *et al.* 2016;  
363 Diaz-Manzano *et al.* 2018; Medina *et al.*, 2017).

### 364 **miR408 and miR398: two copper-responsive microRNA families activated in galls** 365 **induced by *M. incognita***

366 Sequencing of small RNAs showed that mature miR408 and miR398b/c microRNAs  
367 accumulated in galls at 7 and/or 14 dpi, compared to uninfected roots, in both *A. thaliana*  
368 (Medina *et al.*, 2017) and *S. lycopersicum*. A combination of *in silico* predictions of the  
369 transcripts targeted by miR408 and transcriptional analyses of galls and uninfected roots  
370 identified the *UCLACYANIN-2 (UCC2)* and the *PHOSPHATASE (PP2CG)* genes as two  
371 putative targets of miR408 downregulated in galls. The cleavage of *UCC2* transcripts by  
372 miR408 has been biologically validated in *Arabidopsis* and rice (Thatcher *et al.*, 2015; Zhang  
373 *et al.*, 2017). Moreover, several targets of miR398 have been biologically validated, including  
374 the cytosolic *CSD1* and chloroplastic *CSD2*, and the non-canonical target *BCBP* (Beauclair *et*  
375 *al.*, 2010; Brousse *et al.*, 2014). Our analysis, thus, identified several biologically validated and  
376 conserved targets that may be considered robust candidates for mediating the functions of  
377 miR398b/c and miR408 in galls.

378 The inactivation of miR408 in *Arabidopsis* T-DNA mutant lines, or of miR398b/c function in  
379 transgenic plants expressing mutated *CSD1* or *BCBP* resistant to miR398 cleavage, led to  
380 decreases in both the parameters used to assess parasitic success (the number of galls and the  
381 number of females producing egg masses per root). The smaller number of galls in the mutant  
382 lines demonstrates that miR398 family and miR408 promote infection in the early plant

383 response to RKN. Moreover, the smaller feeding sites observed in the two *miR408* KO lines  
384 and the *spl7* mutant demonstrate that this miR408 and SPL7 promote the development of the  
385 giant cells, which are essential for nematode growth and development. Females are unable to  
386 develop normally if the feeding cells are too small, as already reported in some *Arabidopsis*  
387 mutants, such as lines with a knockout of *PHYTOSULFOKINE RECEPTOR1 (PSKR1)* (Rodiuc  
388 *et al.*, 2016). Only a few genes and plant functions have been demonstrated to be essential for  
389 the formation of giant feeding cells (Favery *et al.*, 2020). In the absence of changes in giant cell  
390 size in the *mcsd1* and *mbcbp* mutants, we hypothesise that the miR398-regulated *CSD1* and  
391 *BCBP* genes may play a role in giant cell functioning, potentially in reactive oxygen species  
392 (ROS)-related redox regulation and signalling (Zhao *et al.*, 2020). Further studies will be  
393 required to determine their precise roles in the plant-RKN interaction.

#### 394 **SPL7 is a regulator of miR408 and miR398 in galls**

395 In *A. thaliana*, it has been shown that *MIR408*, *MIR398B* and *MIR398C* are activated by the  
396 same transcription factor, SPL7, the activity of which is dependent on copper levels (Yamasaki  
397 *et al.*, 2009; Araki *et al.*, 2018). We confirmed the activity of the *SPL7* promoter and *MIR408*  
398 in feeding cells and neighbouring cells. The co-expression of *SPL7* and *MIR408* within  
399 developing galls, and the similar nematode infection phenotype, with feeding site formation  
400 defects, strongly suggest that *SPL7* is responsible for activating *MIR408* transcription in galls,  
401 as already reported in leaves and the root vasculature (Yamasaki *et al.*, 2009; Araki *et al.*, 2018).  
402 We therefore hypothesised that the expression of *MIR408* and *MIR398B* and *-C* is activated by  
403 the *SPL7* transcription factor in response to a decrease in copper concentration within galls.  
404 Other transcription factors, such as HY5 and PIF1, which are known to regulate the expression  
405 of *MIR408* in response to light stress (Zhang *et al.*, 2014; Jiang *et al.*, 2021), are expressed in  
406 galls and could also play a role in the regulation of *MIR408* expression. The strong repression  
407 of *MIR408* by excess copper observed in galls suggests that *MIR408* upregulation in galls is  
408 predominantly driven by copper and SPL7. However, we can't exclude that nematode effectors  
409 may also influence directly the expression of *MIR408* and *MIR398* in addition to the regulation  
410 by copper modulation. Further analyses are now required to understand how these microRNAs  
411 are induced in response to nematode infection.

412

#### 413 **Modulation of copper levels, a key conserved factor for gall formation**

414 Infection assays on *A. thaliana* plants watered with a copper sulphate solution at a concentration  
415 non-toxic for plants and nematodes, showed a strong decreased RKN infection rates and  
416 resulted in defective feeding site formation. Together with the upregulation in galls of two  
417 microRNA families known to be induced by copper deficiency, the miR408 and miR398  
418 families, and the regulation of *MIR408* expression by copper, this finding suggests that copper  
419 content decreases in the galls induced by RKN infection. This hypothesis is supported by the  
420 downregulation of the *COPT2* gene, encoding a copper importer, in the *Arabidopsis* gall  
421 transcriptome (Jammes *et al.*, 2005). Micronutrients quantifications have also demonstrated a  
422 decrease in copper concentration in RKN-infected susceptible tomato roots (Lobna *et al.*, 2017).

423 The ***SPL7/MIR408-UCC2/MIR398-CSD1* copper module** may be a key factor in gall  
424 formation, conserved across the plant kingdom. MiR408 and miR398 have been identified in  
425 more than 40 plant species (Griffiths-Jones *et al.*, 2007) and *SPL7* is widely conserved  
426 throughout the plant kingdom (Yamasaki *et al.*, 2009). Moreover, the targeting of  
427 *UCLACYANIN2* by miR408 and of *CSD1* by miR398 is conserved in both dicotyledonous and  
428 monocotyledonous plants (Zhang *et al.*, 2017; Thatcher *et al.*, 2015). miR408 and miR398  
429 targets are associated with lignin metabolism either directly like *UCC2* (Reyt *et al.*, 2020) or  
430 indirectly like *CSD1* via the ROS. Cell wall lignin is restructured during the development of  
431 the feeding cells and galls are subject to extensive changes in vascularization, resulting in the  
432 giant cells being engaged within a network of *de novo* formed xylem and phloem cells (Bartlem,  
433 Kones and Hammes, 2014). Therefore miR398 and miR408 may be involved in modification  
434 of feeding cell wall lignin or lignin network within galls. Moreover, a role for UCLACYANINS  
435 in the formation of a lignified nanodomain within the Casparian strips known to form an  
436 endodermal barrier in *Arabidopsis* roots has recently been described (Reyt *et al.*, 2020).  
437 Casparian strip defects have been observed in the endodermis bordering the giant cell area  
438 within sorghum galls induced by *M. naasi* (Ediz and Dickerson, 1976). Moreover, *Arabidopsis*  
439 mutants with disrupted Casparian strips are particularly susceptible to RKN (Holbein *et al.*,  
440 2019). The infection of plants with nematodes may, therefore, provides a unique model for  
441 investigating the role of copper modulation, via microRNAs and its targets, in the formation of  
442 Casparian strips.

#### 443 **Acknowledgements**

444 We would like to thank Dr. Nicolas Bouché (INRAE Versailles, France) for helpful discussions  
445 and for providing the *mcbcbp* and *mcsd1* *Arabidopsis* lines. We would like to thank Dr. Lei Li

446 (Beijing University, China) for providing the *pMIR408:GUS Arabidopsis* line. We would also  
447 like to thank Dr. Toshiharu Shikanai (Kyoto University, Japan) for providing the *pSPL7:GUS*  
448 and *ko spl7 Arabidopsis* lines. The microscopy work was performed at the SPIBOC imaging  
449 facility of Institut Sophia Agrobiotech. We thank Dr Olivier Pierre and the entire team of the  
450 platform for assistance with microscopy. This work was funded by the INRAE SPE department  
451 and the French Government (National Research Agency, ANR) through the ‘Investments for  
452 the Future’ LabEx SIGNALIFE: programme reference #ANR-11-LABX-0028-01 and IDEX  
453 UCAJedi ANR-15-IDEX-0, and by the French-Japanese bilateral collaboration programme  
454 PHC SAKURA 2019 #43006VJ. Y.N. was supported by a doctoral fellowship from Lebanon  
455 (Municipal Council of Aazzée, Lebanon).

#### 456 **Author contribution**

457 YN, S.J.P and B.F. designed the study and wrote the manuscript. Y.N., J.M. and S.J.P. designed  
458 the study and performed the experimental work. All authors analysed and discussed the data.  
459 M.Q. and P.A. participated in the writing of the manuscript. S.T. participated in the copper  
460 studies. MdR analysed NGS data. KM and YN performed the qPCR.

#### 461 **Data availability**

462 The data that support the findings of this study are available from the corresponding author  
463 upon reasonable request.

#### 464 **References:**

- 465 **Abad P, Williamson VM. 2010.** Plant Nematode Interaction: A Sophisticated Dialogue.  
466 *Advances in Botanical Research* **53**: 147–192.
- 467 **de Almeida Engler J, Gheysen G. 2013.** Nematode-induced endoreduplication in plant host  
468 cells: why and how? *Molecular Plant-Microbe Interactions* **26**: 17–24.
- 469 **Araki R, Mermoud M, Yamasaki H, Kamiya T, Fujiwara T, Shikanai T. 2018.** SPL7  
470 locally regulates copper-homeostasis-related genes in Arabidopsis. *Journal of Plant*  
471 *Physiology* **224–225**: 137–143.
- 472 **Axtell MJ. 2013.** Classification and Comparison of Small RNAs from Plants. *Annual Review*  
473 *of Plant Biology* **64**: 137–159.
- 474 **Barciszewska-Pacak M, Milanowska K, Knop K, Bielewicz D, Nuc P, Plewka P, Pacak**

475 **AM, Vazquez F, Karlowski W, Jarmolowski A, et al. 2015.** Arabidopsis microRNA  
476 expression regulation in a wide range of abiotic stress responses. *Frontiers in Plant Science* **6**:  
477 410.

478 **Bartlem DG, Jones MGK and Hammes UZ. 2013.** Vascularization and nutrient delivery at  
479 root-knot nematode feeding sites in host roots. *Journal of Experimental Botany* **65**: 1789-  
480 1798.

481 **Beauclair L, Yu A, Bouché N. 2010.** MicroRNA-directed cleavage and translational  
482 repression of the copper chaperone for superoxide dismutase mRNA in Arabidopsis. *Plant*  
483 *Journal* **62**: 454–462.

484 **Bernal M, Casero D, Singh V, Wilson GT, Grande A, Yang H, Dodani SC, Pellegrini M,**  
485 **Huijser P, Connolly EL, et al. 2012.** Transcriptome sequencing identifies SPL7-regulated  
486 copper acquisition genes FRO4/FRO5 and the copper dependence of iron homeostasis in  
487 Arabidopsis. *Plant Cell* **24**: 738–761.

488 **Blok VC, Jones JT, Phillips MS, Trudgill DL. 2008.** Parasitism genes and host range  
489 disparities in biotrophic nematodes : the conundrum of polyphagy versus specialisation.  
490 *BioEssays* **30**: 249–259.

491 **Brousse C, Liu Q, Beauclair L, Deremetz A, Axtell MJ, Bouché N. 2014.** A non-canonical  
492 plant microRNA target site. *Nucleic Acids Research* **42**: 5270–5279.

493 **Burkhead JL, Gogolin Reynolds KA, Abdel-Ghany SE, Cohu CM, Pilon M. 2009.**  
494 Copper homeostasis. *New Phytologist* **182**: 799–816.

495 **Cabrera J, Bustos R, Favery B, Fenoll C, Escobar C. 2014.** NEMATIC: A simple and  
496 versatile tool for the insilico analysis of plant-nematode interactions. *Molecular Plant*  
497 *Pathology* **15**: 627–636.

498 **Cai Q, Qiao L, Wang M, He B, Lin F-M, Palmquist J, Huang S-D, Jin H. 2018.** Plants  
499 send small RNAs in extracellular vesicles to fungal pathogen to silence virulence genes.  
500 *Science* **360**: 1126–1129.

501 **Caillaud M-C, Favery B. 2016.** In Vivo Imaging of Microtubule Organization in Dividing  
502 Giant Cell. *Methods in molecular biology (Clifton, N.J.)* **1370**: 137–44.

503 **Caillaud M-C, Lecomte P, Jammes F, Quentin M, Pagnotta S, Andrio E, de Almeida**  
504 **Engler J, Marfaing N, Gounon P, Abad P, et al. 2008.** MAP65-3 microtubule-associated  
505 protein is essential for nematode-induced giant cell ontogenesis in Arabidopsis. *The Plant cell*

506 20: 423–37.

507 **Chávez Montes RA, De Fátima Rosas-Cárdenas F, De Paoli E, Accerbi M, Rymarquis**  
508 **LA, Mahalingam G, Marsch-Martínez N, Meyers BC, Green PJ, De Folter S. 2014.**  
509 Sample sequencing of vascular plants demonstrates widespread conservation and divergence  
510 of microRNAs. *Nature Communications* 5: 3722.

511 **Curaba J, Singh MB, Bhalla PL. 2014.** miRNAs in the crosstalk between phytohormone  
512 signalling pathways. *Journal of experimental botany* 65: 1425–38.

513 **Dunker F, Trutzenberg A, Rothenpieler JS, Kuhn S, Pröls R, Schreiber T, Tissier A,**  
514 **Kemen A, Kemen E, Hückelhoven R, et al. 2020.** Oomycete small RNAs bind to the plant  
515 RNA-induced silencing complex for virulence. *eLife* 9 :e56096.

516 **Ediz SA, Dickerson OJ. 1976.** Life cycle, pathogenicity, histopathology, and host range of  
517 race 5 of the barley root-knot nematode. *Journal of Nematology* 8: 228–231.

518 **Escobar C, Barcala M, Cabrera J, Fenoll C. 2015.** Overview of root-knot nematodes and  
519 giant cells. *Advances in Botanical Research* 73: 1–32.

520 **Escobar C, Brown S, Mitchum MG. 2011.** Transcriptomic and Proteomic Analysis of the  
521 Plant Response to Nematode Infection. In: Jones J, Gheysen G, Fenoll C, eds. Genomics and  
522 Molecular Genetics of Plant-Nematode Interactions. Dordrecht: Springer Netherlands, 157–  
523 173.

524 **Favery B, Dubreuil G, Chen M-S, Giron D, Abad P. 2020.** Gall-Inducing Parasites:  
525 Convergent and Conserved Strategies of Plant Manipulation by Insects and Nematodes.  
526 *Annual Review of Phytopathology* 58: 1–22.

527 **Favery B, Lecomte P, Gil N, Bechtold N, Bouchez D, Dalmaso A, Abad P. 1998.** RPE, a  
528 plant gene involved in early developmental steps of nematode feeding cells. *The EMBO*  
529 *journal* 17: 6799–811.

530 **Fu Y, Mason AS, Zhang Y, Lin B, Xiao M, Fu D, Yu H. 2019.** MicroRNA-mRNA  
531 expression profiles and their potential role in cadmium stress response in Brassica napus.  
532 *BMC Plant Biology* 19: 570.

533 **Griffiths-Jones S, Saini HK, van Dongen S, Enright AJ. 2007.** miRBase: tools for  
534 microRNA genomics. *Nucleic Acids Research* 36: D154–D158.

535 **Hoang NT, Tóth K, Stacey G. 2020.** The role of microRNAs in the legume–Rhizobium  
536 nitrogen-fixing symbiosis (R Mittler, Ed.). *Journal of Experimental Botany* 71: 1668–1680.

537 **Holbein J, Franke RB, Marhavý P, Fujita S, Górecka M, Sobczak M, Geldner N,**  
538 **Schreiber L, Grundler FMW, Siddique S. 2019.** Root endodermal barrier system  
539 contributes to defence against plant-parasitic cyst and root-knot nematodes. *Plant Journal*  
540 **100:** 221–236.

541 **Hutvágner G, McLachlan J, Pasquinelli AE, Bálint É, Tuschl T, Zamore PD. 2001.** A  
542 cellular function for the RNA-interference enzyme dicer in the maturation of the let-7 small  
543 temporal RNA. *Science* **293:** 834–8.

544 **Jammes F, Lecomte P, Almeida-Engler J, Bitton F, Martin-Magniette M-LL, Renou JP,**  
545 **Abad P, Favery B, De Almeida-Engler J, Bitton F, et al. 2005.** Genome-wide expression  
546 profiling of the host response to root-knot nematode infection in Arabidopsis. *The Plant*  
547 *Journal* **44:** 447–458.

548 **Jaubert-Possamai S, Noureddine Y, Favery B. 2019.** MicroRNAs, New Players in the  
549 Plant–Nematode Interaction. *Frontiers in Plant Science* **10:** 1–8.

550 **Jiang A, Guo Z, Pan J, Yang Y, Zhuang Y, Zuo D, Hao C, Gao Z, Xin P, Chu J, et al.**  
551 **2021.** The PIF1-miR408-PLANTACYANIN repression cascade regulates light-dependent  
552 seed germination. *Plant Cell* **33:** 1506–1529.

553 **Kuo Y-W, Lin J-S, Li Y-C, Jhu M-Y, King Y-C, Jeng S-T. 2019.** MicroR408 regulates  
554 defense response upon wounding in sweet potato. *Journal of Experimental Botany* **70:** 469–  
555 483.

556 **Lobna H, Aymen EM, Hajer R, Naima M-B, Najet H-R. 2017.** Biochemical and plant  
557 nutrient alterations induced by *Meloidogyne javanica* and *Fusarium oxysporum* f.sp.radicis  
558 lycopersici co-infection on tomato cultivars with differing level of resistance to *M. javanica*.  
559 *European Journal of Plant Pathology* **148:** 463–472.

560 **Ma C, Burd S, Lers A. 2015.** miR408 is involved in abiotic stress responses in Arabidopsis.  
561 *The Plant Journal* **84:** 169–187.

562 **Maunoury N, Vaucheret H. 2011.** AGO1 and AGO2 Act Redundantly in miR408-Mediated  
563 Plantacyanin Regulation (M Bendahmane, Ed.). *PLoS ONE* **6:** e28729.

564 **Medina C, da Rocha M, Magliano M, Ratpopoulo A, Revel B, Marteu N, Magnone V,**  
565 **Lebrigand K, Cabrera J, Barcala M, et al. 2017.** Characterization of microRNAs from  
566 Arabidopsis galls highlights a role for miR159 in the plant response to the root-knot nematode  
567 *Meloidogyne incognita*. *New Phytologist* **216:** 882–896.

568 **Reyt G, Chao Z, Flis P, Salas-González I, Castrillo G, Chao D-YY, Salt DE. 2020.**

569 Uclacyanin Proteins Are Required for Lignified Nanodomain Formation within Casparian  
570 Strips. *Current Biology* **30**: 4103-4111.e6.

571 **Rodiuc N, Barlet X, Hok S, Perfus-Barbeoch L, Allasia V, Engler G, Séassau A, Marteu**  
572 **N, de Almeida-Engler J, Panabières F, et al. 2016.** Evolutionarily distant pathogens require  
573 the Arabidopsis phytoalexin signalling pathway to establish disease. *Plant, Cell &*  
574 *Environment* **39**: 1396–1407.

575 **Schulman BRM, Esquela-Kerscher A, Slack FJ. 2005.** Reciprocal expression of lin-41 and  
576 the microRNAs let-7 and mir-125 during mouse embryogenesis. *Developmental Dynamics*  
577 **234**: 1046-54.

578 **Schulten A, Bytomski L, Quintana J, Bernal M, Krämer U. 2019.** Do Arabidopsis  
579 Squamosa promoter binding Protein-Like genes act together in plant acclimation to copper or  
580 zinc deficiency? *Plant Direct* **3**: 590182.

581 **Sommer F, Kropat J, Malasarn D, Grosseohme NE, Chen X, Giedroc DP, Merchant SS.**  
582 **2011.** The CRR1 Nutritional Copper Sensor in Chlamydomonas Contains Two Distinct  
583 Metal-Responsive Domains. *The Plant Cell* **22**: 4098–4113.

584 **Thatcher SR, Burd S, Wright C, Lers A, Green PJ. 2015.** Differential expression of  
585 miRNAs and their target genes in senescing leaves and siliques: Insights from deep  
586 sequencing of small RNAs and cleaved target RNAs. *Plant, Cell and Environment* **38**: 188–  
587 200.

588 **Thomson JM, Newman M, Parker JS, Morin-Kensicki EM, Wright T, Hammond SM.**  
589 **2006.** Extensive post-transcriptional regulation of microRNAs and its implications for cancer.  
590 *Genes and Development* **20**: 2202-7.

591 **Weiberg A, Jin H. 2015.** Small RNAs—the secret agents in the plant–pathogen interactions.  
592 *Current Opinion in Plant Biology* **26**: 87–94.

593 **Weiberg A, Wang M, Lin F-M, Zhao H, Zhang Z, Kaloshian I, Huang H-D, Jin H. 2013.**  
594 Fungal Small RNAs Suppress Plant Immunity by Hijacking Host RNA Interference  
595 Pathways. *Science* **342**: 118–123.

596 **Wiggers RJJ, Starr JLL, Price HJJ. 1990.** DNA content and variation in chromosome  
597 number in plant cells affected by *Meloidogyne incognita* and *M. arenaria*. *Phytopathology* **80**:  
598 1391–1395.

599 **Xu W, Meng Y, Wise RP. 2014.** Mla- and Rom1-mediated control of microRNA398 and

600 chloroplast copper/zinc superoxide dismutase regulates cell death in response to the barley  
601 powdery mildew fungus. *New Phytologist* **201**: 1396–1412.

602 **Yamaguchi YL, Suzuki R, Cabrera J, Nakagami S, Sagara T, Ejima C, Sano R, Aoki Y,**  
603 **Olmo R, Kurata T, et al. 2017.** Root-Knot and Cyst Nematodes Activate Procambium-  
604 Associated Genes in Arabidopsis Roots. *Frontiers in Plant Science* **8**: 1–13.

605 **Yamasaki H, Abdel-Ghany SE, Cohu CM, Kobayashi Y, Shikanai T, Pilon M. 2007.**  
606 Regulation of copper homeostasis by micro-RNA in Arabidopsis. *Journal of Biological*  
607 *Chemistry* **282**: 16369–16378.

608 **Yamasaki H, Hayashi M, Fukazawa M, Kobayashi Y, Shikanai T. 2009.** SQUAMOSA  
609 promoter binding protein-like7 is a central regulator for copper homeostasis in Arabidopsis.  
610 *Plant Cell* **21**: 347–361.

611 **Zhang H, Li L. 2013.** SQUAMOSA promoter binding protein-like7 regulated microRNA408  
612 is required for vegetative development in Arabidopsis. *Plant Journal* **74**: 98–109.

613 **Zhang J-P, Yu Y, Feng Y-Z, Zhou Y-F, Zhang F, Yang Y-W, Lei M-Q, Zhang Y-C,**  
614 **Chen Y-Q. 2017.** MiR408 Regulates Grain Yield and Photosynthesis via a Phytocyanin  
615 Protein. *Plant Physiology* **175**: 1175–1185.

616 **Zhang H, Zhao X, Li J, Cai H, Deng XW, Li L. 2014.** Microrna408 is critical for the HY5-  
617 SPL7 gene network that mediates the coordinated response to light and copper. *Plant Cell* **26**:  
618 4933–4953.

619 **Zhao J, Mejias J, Quentin M, Chen Y, de Almeida-Engler J, Mao Z, Sun Q, Liu Q, Xie**  
620 **B, Abad P, et al. 2020.** The root-knot nematode effector MiPDI1 targets a stress-associated  
621 protein (SAP) to establish disease in Solanaceae and Arabidopsis. *New Phytologist* **228**:  
622 1417–1430.

623  
624  
625  
626  
627  
628

## 629 **Supporting Information**

630 **Fig. S1** Localisation of pMIR408 activity in fully developed galls of *Arabidopsis thaliana*.

631 **Fig S2** Relative quantification of premiR408 and of *UCC2* and *PP2G* transcripts by qPCR in  
632 galls in comparison to uninfected *Arabidopsis thaliana* roots at 7 and 14 dpi

633 **Fig. S3** Root phenotype of the *mir408-1* and *mir408-2* *Arabidopsis thaliana* KO lines.

634 **Fig. S4** Root phenotype of the *spl7* *Arabidopsis thaliana* KO line.

635 **Fig. S5** Relative quantification of premiR398b/c and of *CSD1*, *CSD2* and *BCBP* transcripts by  
636 qPCR in galls in comparison to uninfected *Arabidopsis thaliana* roots at 7 and 14 dpi.

637 **Fig. S6.** Root phenotype and area covered by the feeding site in the *mcsd1* and *mbcbp*  
638 *Arabidopsis thaliana* lines.

639 **Fig. S7** Assessment of copper toxicity in *Meloidogyne incognita* J2s.

640 **Fig. S8** Repression of pMIR408 activity in *Arabidopsis thaliana* galls by watering with  
641 CuSO<sub>4</sub>, assessed at 14 days post infection (dpi).

642 **Fig. S9** Root phenotype of *Arabidopsis thaliana* Col0 watered with 50 µM copper sulphate.

643 **Fig. S10** NBT staining of O<sup>2-</sup> on 14 dpi *Arabidopsis thaliana* gall sections.

644 **Table S1** Primers used in qPCR.

645 **Table S2** Expression level of mature sequence of the miR408 and miR398 families  
646 upregulated in *Arabidopsis thaliana* and tomato (*Solanum lycopersum*) galls.

647 **Table S3:** Infection assays with *mir408-1* and *mir408-2* *Arabidopsis thaliana* ko lines  
648 infected with *Meloidogyne incognita*.

649 **Table S4 :** Prediction of *Arabidopsis thaliana* miR408 targets with psRNA targets and  
650 expression profile of these targets in *Arabidopsis thaliana* galls.

651 **Table S5** : Relative quantification of premiR408 and of *UCC2* and *PP2G* transcripts by  
652 qPCR in galls in comparison to uninfected *Arabidopsis thaliana* roots at 7 and 14 dpi.

653 **Table S6** : Infection assays with *spl7-1 Arabidopsis thaliana* lines infected with *Meloidogyne*  
654 *incognita*.

655 **Table S7** : Relative quantification of premiR398b/c and of *CSD1*, *CSD2* and *BCBP*  
656 transcripts by qPCR in galls in comparison to uninfected *Arabidopsis thaliana* roots at 7 and  
657 14 dpi.

658 **Table S8** : Infection assays with *mbcbp* and *mcsd1 Arabidopsis thaliana* lines infected with  
659 *Meloidogyne incognita*.

660 **Table S9** : *Meloidogyne incognita* second stage juvenile (J2) survival after being incubated  
661 for 24 hours in a CuSO<sub>4</sub> solution.

662 **Table S10** : Infection assays of *Meloidogyne incognita* Col0 watered with 50 μM CuSO<sub>4</sub> or  
663 tap water.

664 **Methods S1** Biological Materials, Growth Conditions

665 **Methods S2** RNA extraction

666 **Methods S3** RNA sequencing

667 **Methods S4** miRNAs Analysis

668 **Methods S5** mRNA sequencing

669 **Methods S6** mRNA Analysis

670 **Methods S7** NBT staining

671

672

673

674 **Table & Figures**

675 **Table 1.** Expression profile of miRNAs of the miR408 and miR398 families in *Arabidopsis*  
 676 *thaliana* and tomato galls.

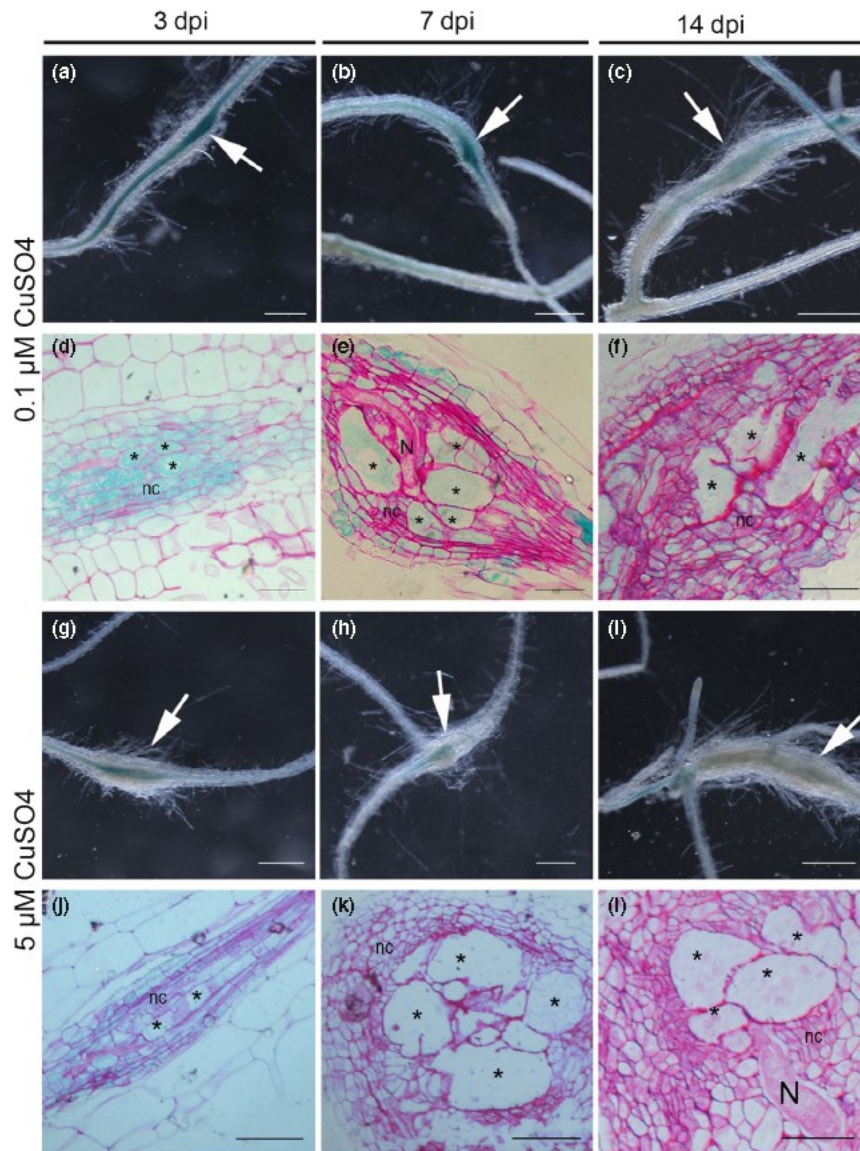
miRNA family	miRNA name	Plant species	miRNA mature sequence	logFC G/R 7dpi	adj. pvalue	logFC G/R 14dpi	adj. pvalue
mir408	SL3.0ch01_346	<i>S. lycopersicum</i>	TGCACAGCCTCTTCCCTGGCT	3,741	0,000	3,289	0,017
	SL3.0ch01_419	<i>S. lycopersicum</i>	TGCACTGCCTCTTCCCTGGCT	1,287	0,029	3,133	0,033
	Ath-miR408	<i>A. thaliana</i>	ATGCACTGCCTCTTCCCTGGC	2,042	0,042	2,411	0,001
mir398	SL3.0ch12_14_3	<i>S. lycopersicum</i>	ATGTGTTCTCAGGTTACCCCT	3,272	0,009	2,166	0,066
	SL3.0ch05_225	<i>S. lycopersicum</i>	TTGTGTTCTCAGGTCACCCCT	0,290	0,863	3,430	0,015
	SL3.0ch11_437	<i>S. lycopersicum</i>	TATGTTCTCAGGTCGCCCTG	2,144	0,112	1,759	0,067
	ath-miR398b-c	<i>A. thaliana</i>	TGTGTTCTCAGGTCACCCCT	2,464	0,119	3,287	0,000

677  
 678 For each miRNA family, the reference in *Arabidopsis* (Ath-miR) and in *Solanum lycopersicum*  
 679 (SL3.0ch) genomes is indicated. The sequence of the mature sequence, the log<sub>2</sub> of the  
 680 Gall/uninfected root expression fold change (Log<sub>2</sub>FC G/R) and statistical significance  
 681 according to the Benjamini Hochberg adjustment (adj. pvalue) for the differentially expressed  
 682 miRNAs at 7 and 14 days post infection (dpi) are indicated. MicroRNAs statistically  
 683 upregulated in galls in comparison to uninfected roots are underlined in red.

684

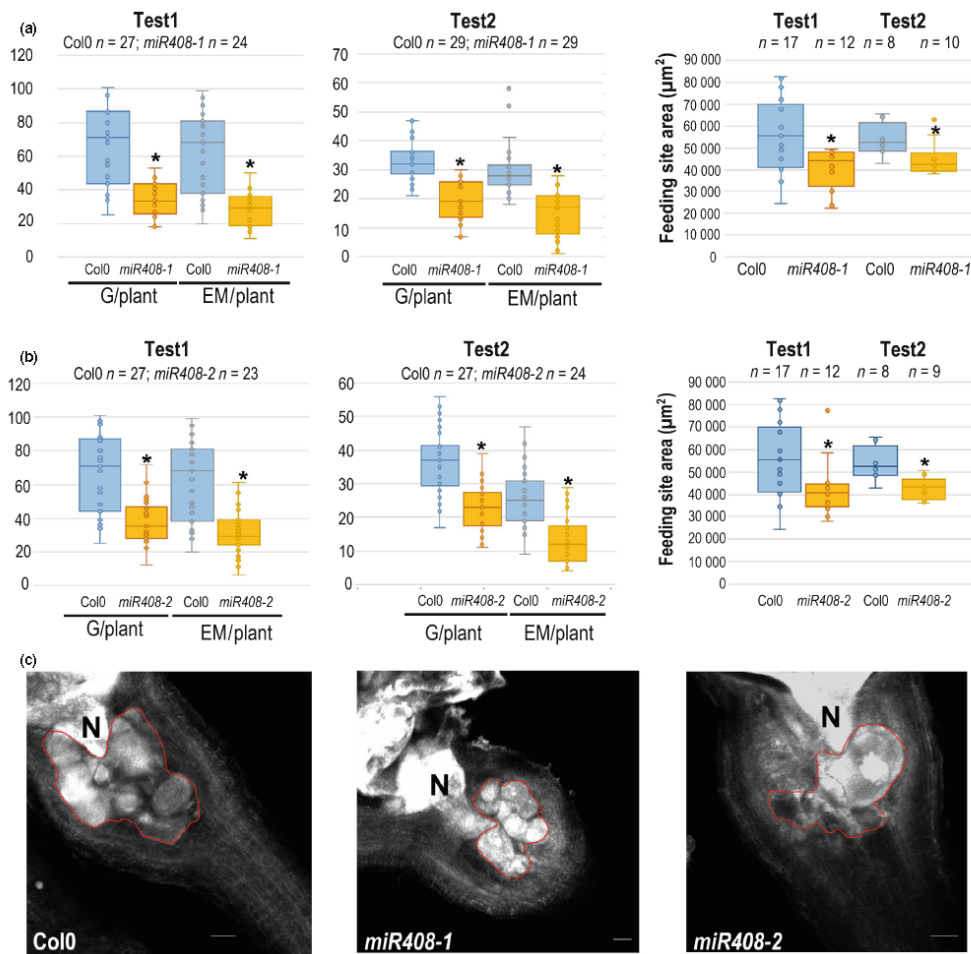
685

686



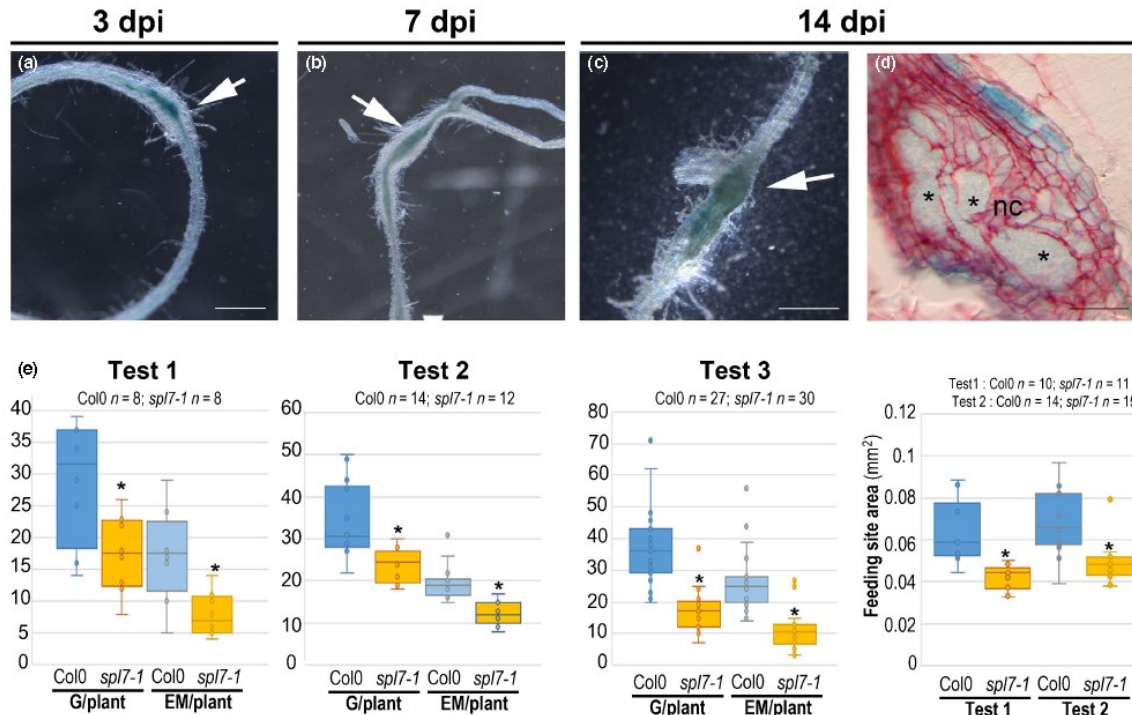
687

688 **Figure 1.** Copper modulates *MIR408* promoter activity in galls. (a-h), The activity of the  
689 *MIR408* promoter was analysed in galls induced by *M. incognita* in *Arabidopsis thaliana*  
690 expressing the *pMIR408::GUS* construct grown in the presence of normal concentrations of  
691 copper (0.1  $\mu\text{M}$   $\text{CuSO}_4$ )(a-f) or in the presence of high concentrations of copper (5.0  $\mu\text{M}$   
692  $\text{CuSO}_4$ )(g-l). (a-c), a strong blue coloration reflecting GUS activity was observed in galls 3  
693 days post infection (dpi) (a), 7 dpi (b) and 14 dpi (c) in plants grown with 0.1  $\mu\text{M}$   $\text{CuSO}_4$ . D-  
694 F, Section of galls at 3 dpi (d), 7dpi (e) and 14 dpi (f) showing the GUS blue signal in giant  
695 cells and in the cells surrounding the giant cells. (g-i), a weaker GUS signal was observed in  
696 galls from plants grown with 5.0  $\mu\text{M}$   $\text{CuSO}_4$  analysed at 3 dpi (g) and 7 dpi (h) and no GUS  
697 signal was observed in galls at 14 dpi (i). (j-l), Section of gall at 3 dpi (j), 7dpi (k) and 14 dpi  
698 (l). Galls are indicated with an arrow; N, nematode; (\*) giant feeding cells; nc, neighbouring  
699 cells. Bars 500  $\mu\text{m}$  (a-c; g-i) or 50  $\mu\text{m}$  (d-f; j-l).



700

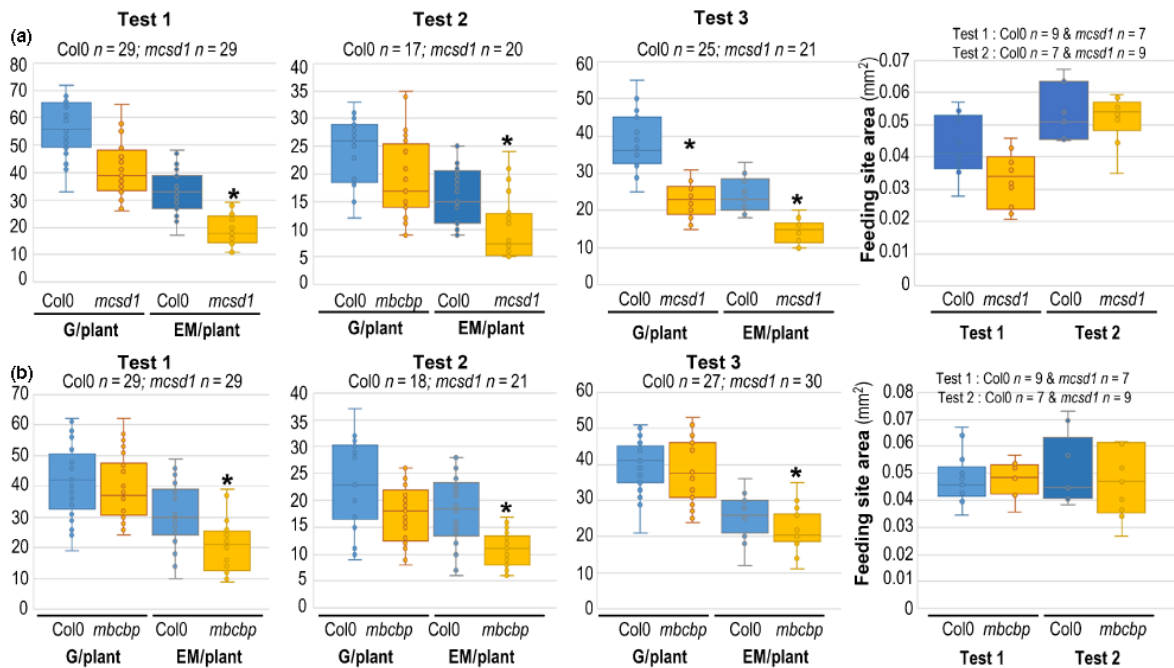
701 **Figure 2:** The *miR408* KO *Arabidopsis thaliana* lines were significantly less susceptible to  
 702 *Meloidogyne incognita* than the wild type. (a-b) The susceptibility of the two *mir408* KO lines,  
 703 *mir408-1* (a) & *mir408-2* (b), and Col0 wild type to *M. incognita* was evaluated by counting  
 704 the number of galls and egg masses per plant (G/plant and EM/plant, respectively) in two  
 705 independent infection assays in soil. (c) The effect of *MIR408* mutation on the development of  
 706 giant feeding cells was further evaluated by measuring the size of the feeding site (circled in  
 707 red) produced in each KO and comparing it to that in Col0. Galls were collected seven weeks  
 708 post *in vitro* infection to measure the area ( $\mu\text{m}^2$ ) covered by the giant cells by the BABB  
 709 clearing method (Cabrera et al., 2018). The impact of plant genotype was analysed in Mann and  
 710 Whitney tests. \*,  $P < 0.05$ . Boxes indicate interquartile range (25th to the 75th percentile). The  
 711 central lines within the boxes represent medians. Whiskers indicate the minimal and maximum  
 712 of the usual values present in the data set. The circle outside the box represents outlier. n : the  
 713 number of plants per line analysed in each assay for the number of galls and egg masses and  
 714 the number of galls per line for each test for measurement of feeding site area. Bars 50 $\mu\text{m}$ . N :  
 715 nematode.



716

717 **Figure 3.** *SPL7* is induced and required for *Meloidogyne incognita* infection and giant cell  
718 formation in *Arabidopsis thaliana*. (a-d), The activity of the *SPL7* promoter (*pSPL7*) was  
719 studied in galls induced by *M. incognita* from *A. thaliana* expressing the *pSPL7::GUS*  
720 construct, at 3 days post inoculation (dpi)(a), 7 dpi (b) and 14 dpi (c). (d), GUS blue staining  
721 was observed within 5.0  $\mu\text{m}$ -thick gall sections at 14 dpi. (e), the KO *spl7* line (SALK093849c)  
722 was infected with *M. incognita* J2. This line was significantly less susceptible to RKN than  
723 Col0, as shown by the smaller mean number of galls and egg masses per plant (G/plant and  
724 EM/plant, respectively) in three independent infection assays. The effect of *spl7* mutation on  
725 the development of feeding cells was further evaluated by measuring the size of the feeding site  
726 area. Galls were collected seven weeks post *in vitro* infection for measurement of the area  
727 ( $\text{mm}^2$ ) covered by the giant cells, by the BABB clearing method (Cabrera et al., 2018). Mann–  
728 Whitney tests were performed for statistical analysis in each experiment; significant differences  
729 relative to Col-0: \*,  $P < 0.05$ . Boxes indicate interquartile range (25th to the 75th percentile).  
730 The central lines within the boxes represent medians. Whiskers indicate the minimal and  
731 maximum of the usual values present in the data set. The circle outside the box represents  
732 outlier. n : the number of plants per line analysed in each assay for the number of galls and egg  
733 masses and the number of galls per line for each test for measurement of feeding site area. Galls  
734 are indicated with an arrow; (\*) giant feeding cells; nc, neighbouring cells. Bars 50  $\mu\text{m}$  (a-c) or  
735 500  $\mu\text{m}$  (d).

736



737

738 **Figure 4.** The miR398-resistant *mcsd1* and *mbcbp* mutant *Arabidopsis thaliana* lines had  
 739 smaller numbers of egg masses. The susceptibility of the (a) *mcsd1* and (b) *mbcbp* lines and of  
 740 wild-type Col0 plants was evaluated by counting the number of galls and egg masses per plant  
 741 (G/plant and EM/plant, respectively) in three independent infection assays in soil. Nematode  
 742 feeding site area (in mm<sup>2</sup>) in wild-type Col0 and *mcsd1* or *mbcbp* mutants were then measured  
 743 following gall clearing with BABB (Cabrera et al., 2018). Results from two independent  
 744 experiments are shown. All data were analysed in Mann and Whitney statistical tests. \*, P <  
 745 0.05. Boxes indicate interquartile range (25th to the 75th percentile). The central lines within  
 746 the boxes represent medians. Whiskers indicate the minimal and maximum of the usual values  
 747 present in the data set. The circle outside the box represents outlier. n : the number of plants per  
 748 line analysed in each assay for the number of galls and egg masses and the number of galls per  
 749 line for each test for measurement of feeding site area.

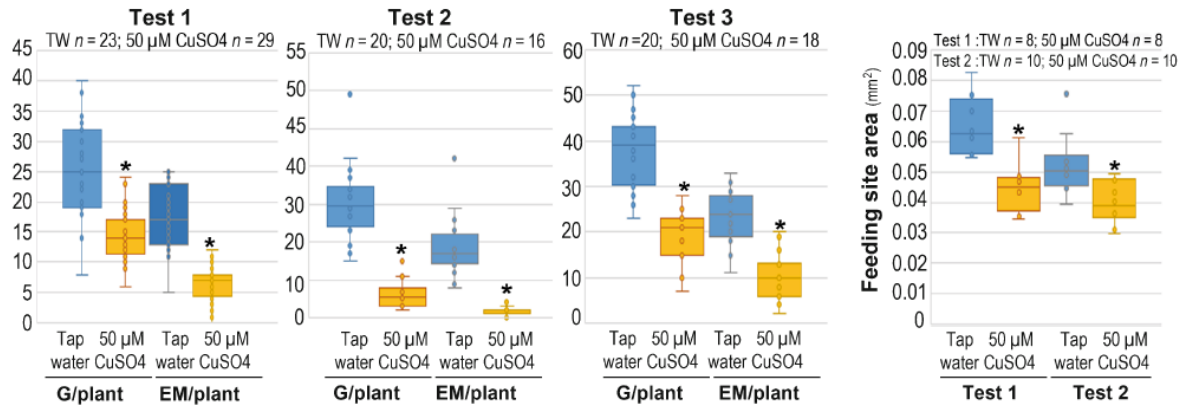
750

751

752

753

754



755

756

757 **Figure 5. *Arabidopsis thaliana* Col0 watered with copper sulphate solution were**  
 758 **significantly less susceptible**

759 to root-knot nematodes. The effect of physiological concentrations of copper on *Meloidogyne*  
 760 *incognita* infection was evaluated by counting galls and egg masses per plant (G/plant and  
 761 EM/plant, respectively) in Col0 plants watered with tap water (TW) or with a copper sulphate  
 762 (CuSO<sub>4</sub>) solution at a non-toxic concentration (50 μM) Three independent experiments were  
 763 performed. Nematode feeding site area (in mm<sup>2</sup>) in wild-type Col0 cultivated on tap water or  
 764 on 50 μM CuSO<sub>4</sub> were then measured following gall clearing with BABB (Cabrera et al., 2018).  
 765 Results from two independent experiments are shown. All data were analysed in Mann and  
 766 Whitney statistical tests. \*, P < 0.05. Boxes indicate interquartile range (25th to the 75th  
 767 percentile). The central lines within the boxes represent medians. Whiskers indicate the minimal  
 768 and maximum of the usual values present in the data set. The circle outside the box represents  
 769 outlier. n : the number of plants per line analysed in each assay for the number of galls and egg  
 770 masses and the number of galls per line in each test for measurement of feeding site area.

771